Electronic Supplementary Material (ESI) for Journal of Materials Chemistry A.
This journal is © The Royal Society of Chemistry 2023

Supplementary Information

Borophene and BC_2N quantum dots heterostructures: Ultrasensitive humidity sensing and multifunctional applications†

Xiang Liu§, Chuang Hou§, Yi Liu, Shifan Chen, Zitong Wu, Xinchao Liang, and Guoan Tai*

State Key Laboratory of Mechanics and Control for Aerospace Structures, Laboratory of Intelligent Nano Materials and Devices of Ministry of Education, College of Aerospace Engineering, Nanjing University of Aeronautics and Astronautics, Nanjing 210016, China
§ Xiang Liu and Chuang Hou contributed equally to this work.

*E-mail: taiguoan@nuaa.edu.cn

This file includes:

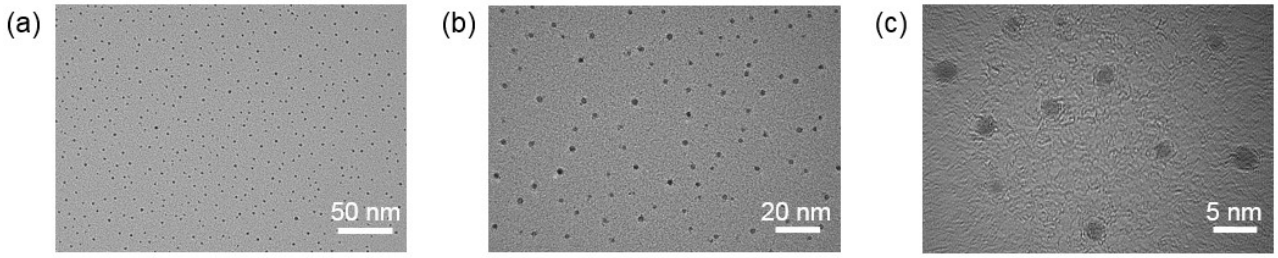

Fig. S1 TEM images of BC_2N QDs.

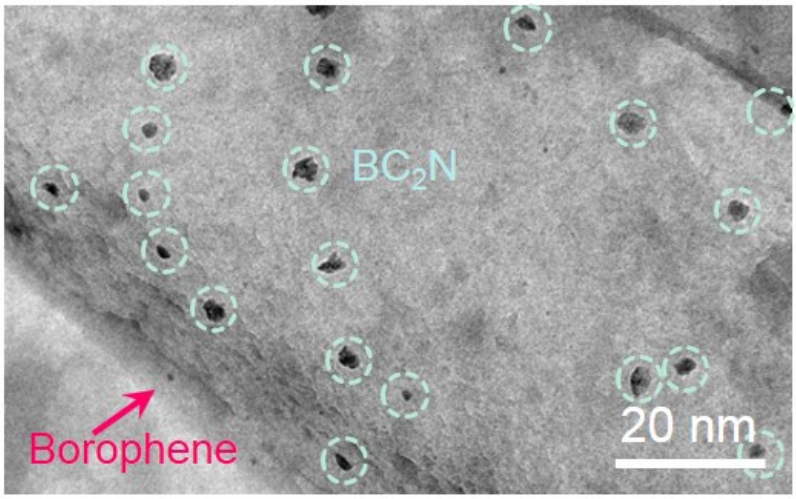

Fig. S2 TEM image of the borophene-BC_2N heterostructures.

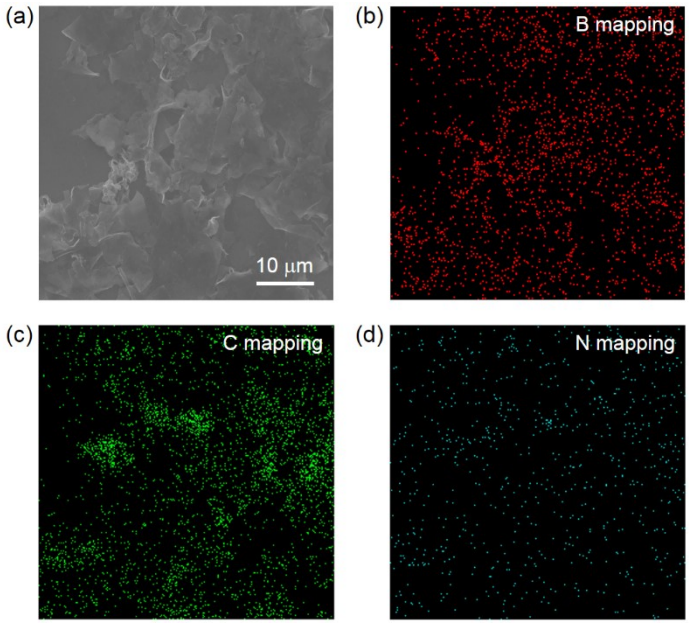

Fig. S3 SEM-mapping of the borophene-BC_2N heterostructures. (a) SEM image of the heterostructures. (b-d) B, C and N elemental mappings of the heterostructures.

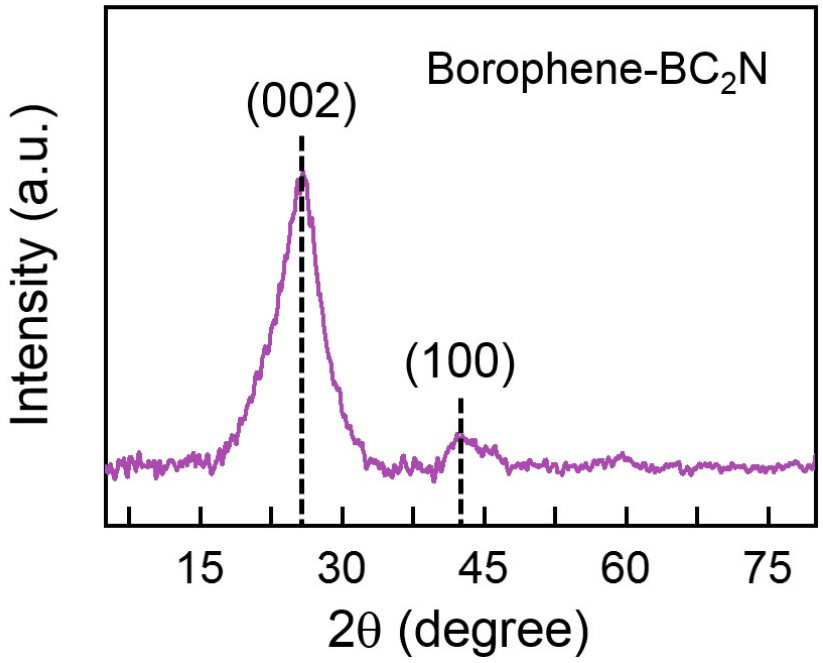

Fig. S4 XRD pattern of the borophene-BC_2N heterostructures.

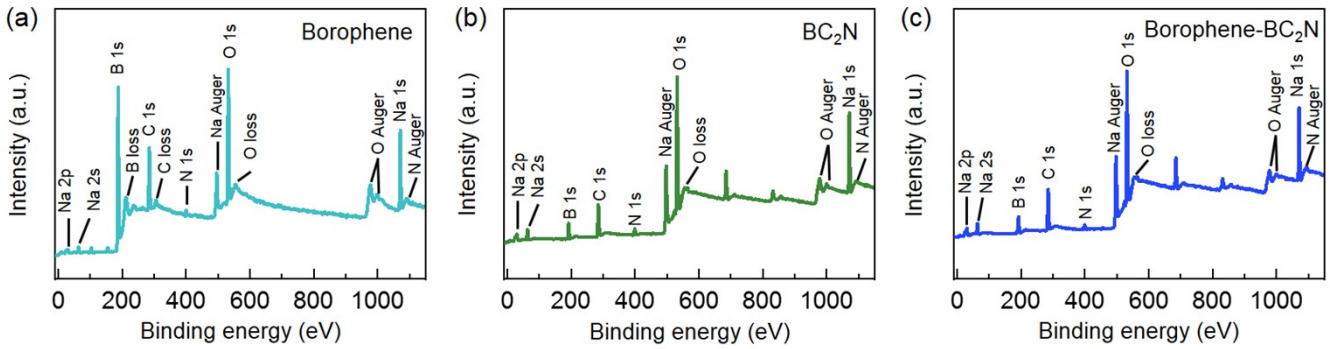

Fig. S5 Full-scale XPS survey of (a) borophene, (b) BC_2N QDs and (c) borophene-BC_2N heterostructures.

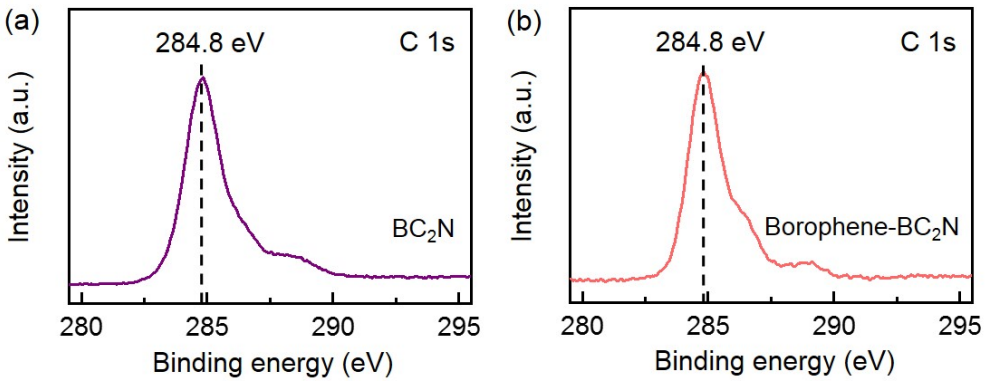

Fig. S6 High resolution spectra of C 1s of (a) BC_2N QDs and (b) borophene-BC_2N heterostructures.

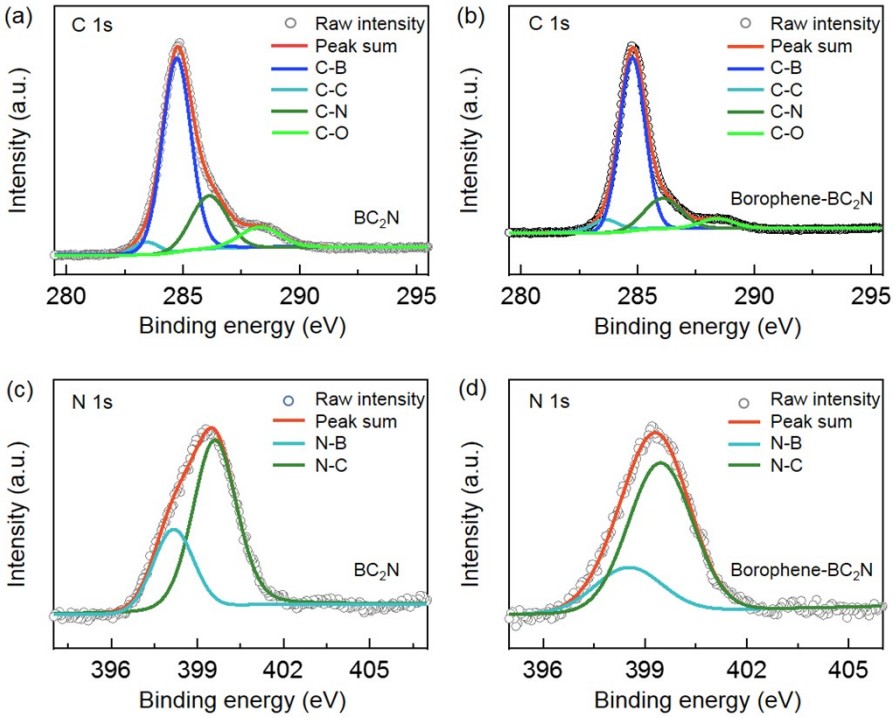

Fig. S7 XPS characterization of BC_2N QDs and borophene-BC_2N heterostructures. (a, b) High-resolution C 1s spectrum of (a) BC_2N QDs and (b) borophene-BC_2N heterostructures. (c, d) High-resolution N 1s spectrum of (c) BC_2N QDs and (d) borophene-BC_2N heterostructures.

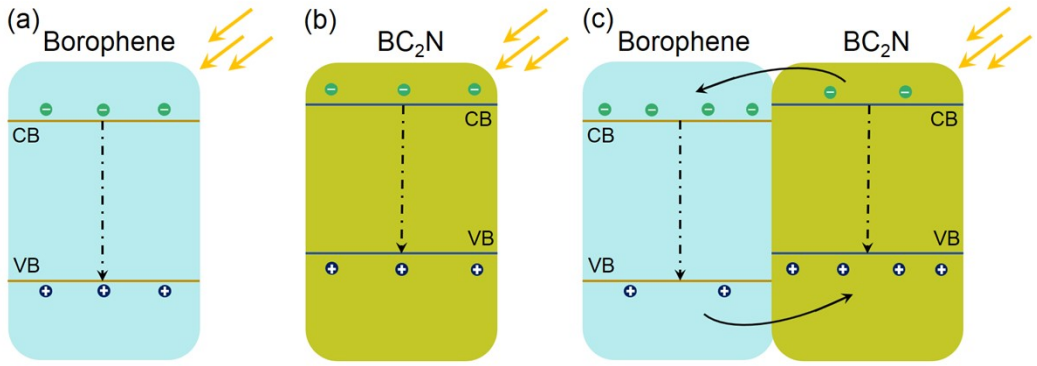

Fig. S8 Schematic illustration of the transfer of photoinduced carriers for (a) borophene, (b) BC_2N QDs and (c) borophene-BC_2N heterostructures.

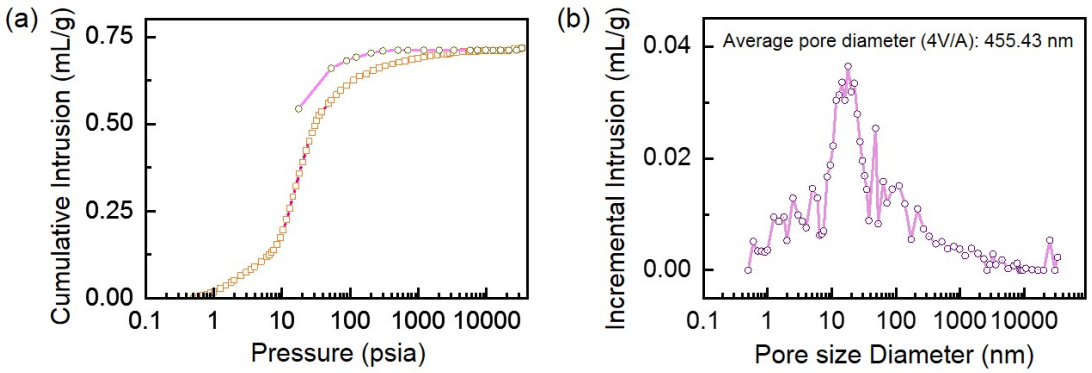

Fig. S9 Intrusion curves and pore size distribution of the borophene-BC_2N heterostructures. (a) Mercury adsorption-desorption isotherm. (b) Pore size distribution curve.

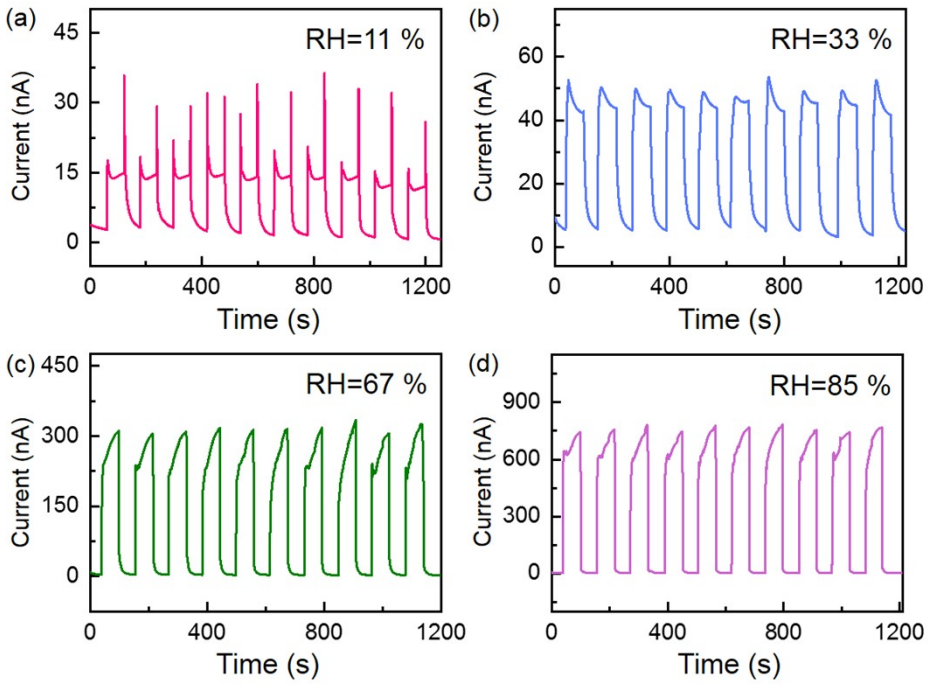

Fig. S10 Cyclic performance of the borophene-BC_2N sensor at (a) 11% RH, (b) 33% RH, (c) 67% RH and (d) 85% RH, respectively.

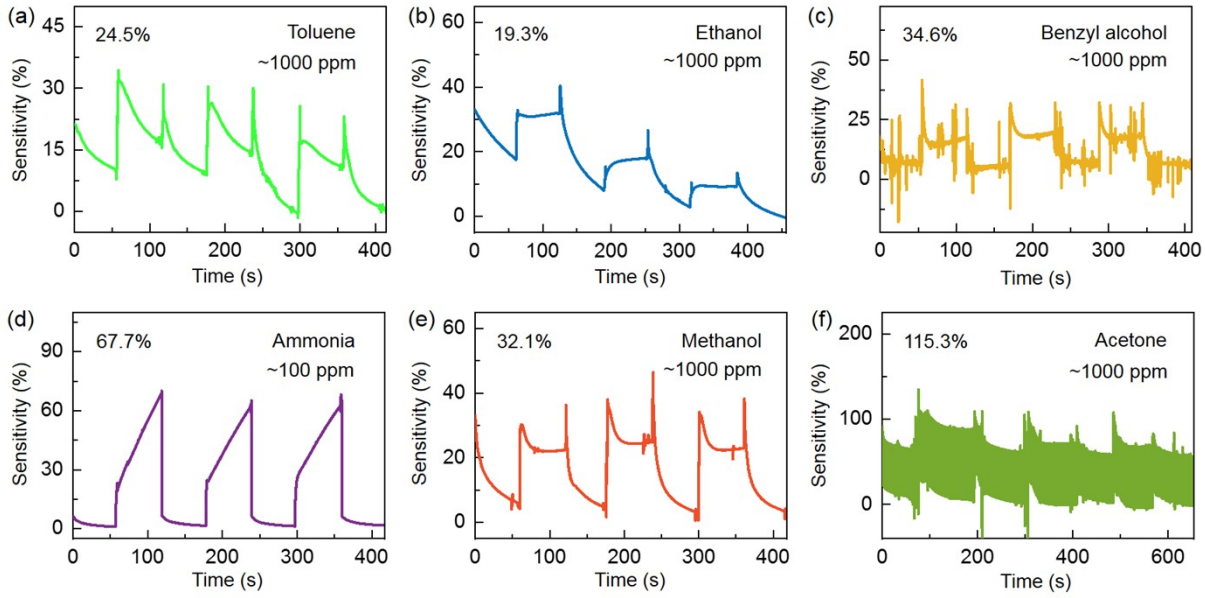

Fig. S11 Response curves of the heterostructured sensor exposed to the typical organic vapors: (a) toluene, (b) ethanol, (c) benzyl alcohol, (d) ammonia, (e) methanol, and (f) acetone.

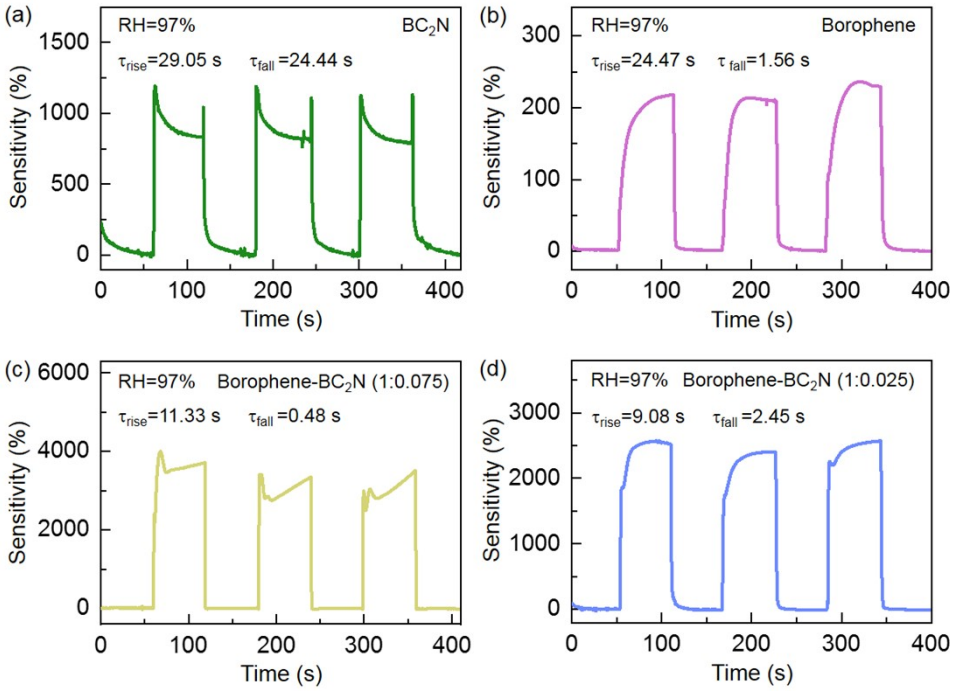

Fig. S12 Response and recovery curves at 97% RH of the sensors based on different samples: (a) BC_2N QDs, (b) borophene, (c) borophene-BC_2N (1:0.075) and (d) borophene-BC_2N (1:0.025).

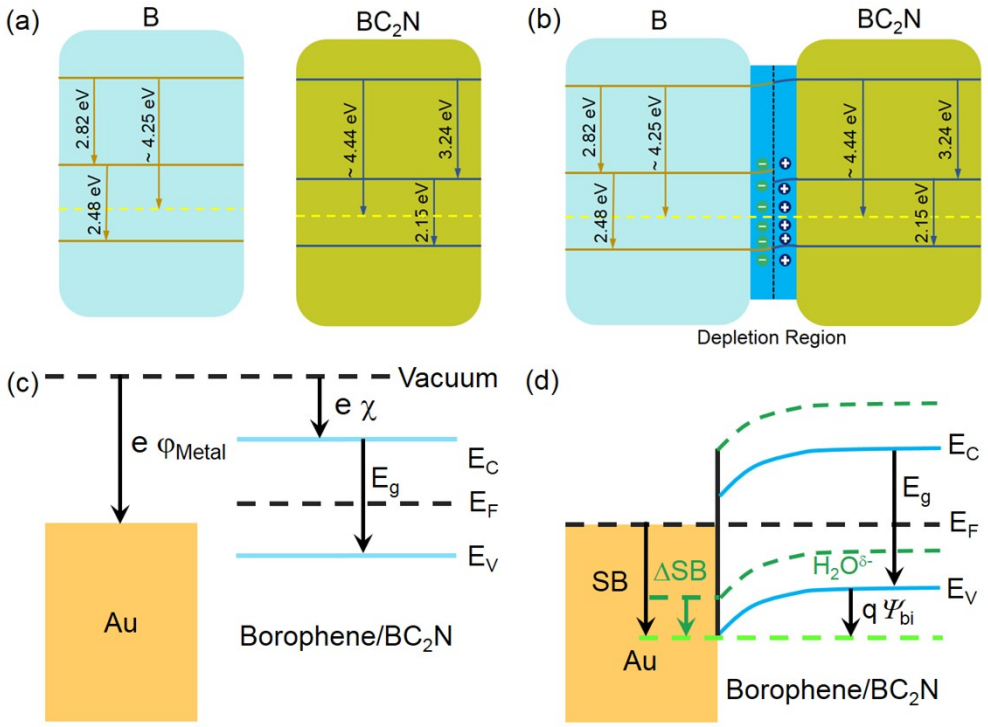

Fig. S13 Analysis of energy band diagram. (a) Band diagram of the borophene and BC_2N before contact. (b) Band realignment of the borophene and BC_2N after contact and the formation of Schottky barrier. (c) Band diagram of the borophene/BC_2N and Au electrode before contact. (d) Band realignment of the borophene/BC_2N and Au electrode after contact and the formation of Schottky barrier, blue and green lines indicate the energy band of the pristine borophene (solid blue), and after exposure to H_2O (dashed green), respectively.

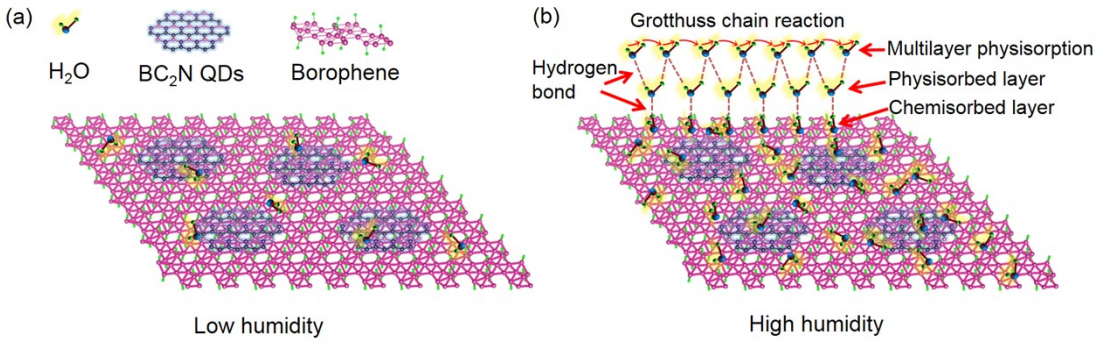

Fig. S14 The H_2O adsorption process on the surface of the borophene-BC_2N heterostructures.

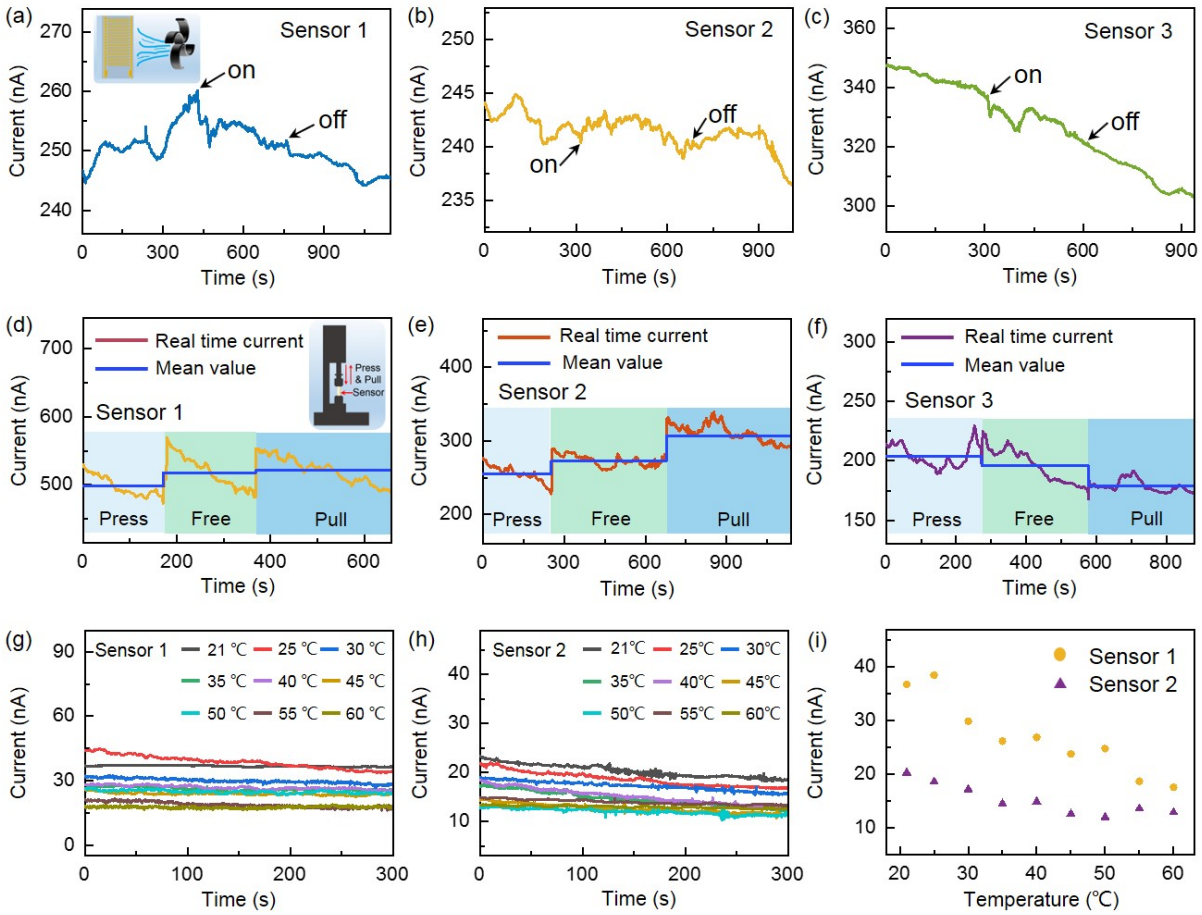

Fig. S15 Responses of the fabricated humidity sensors to the changes of (a-c) wind, (d-f) stress and (g-h) temperature. (i) Relationship between the temperature and the current of the sensors.

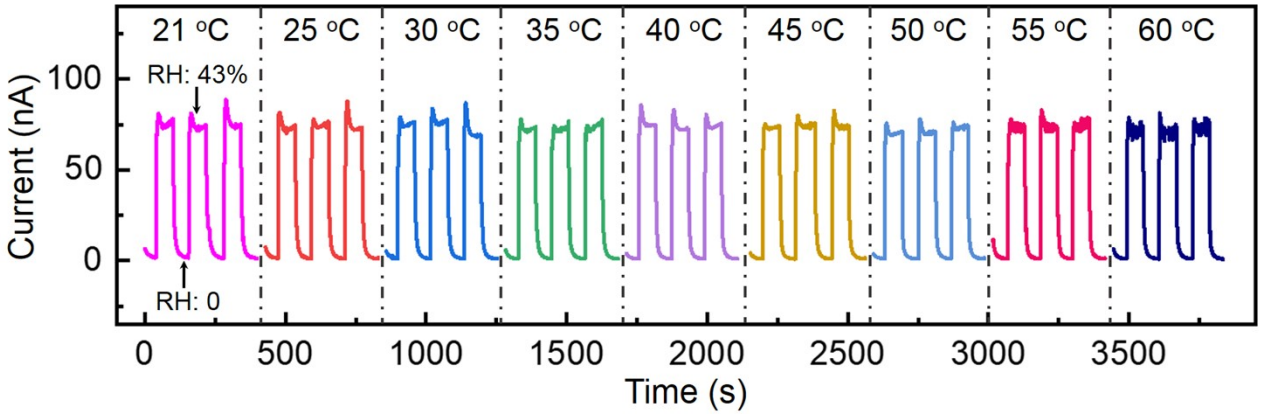

Fig. S16 The response of the humidity sensor to humidity changes (RH: 0%-43%) at different temperature.

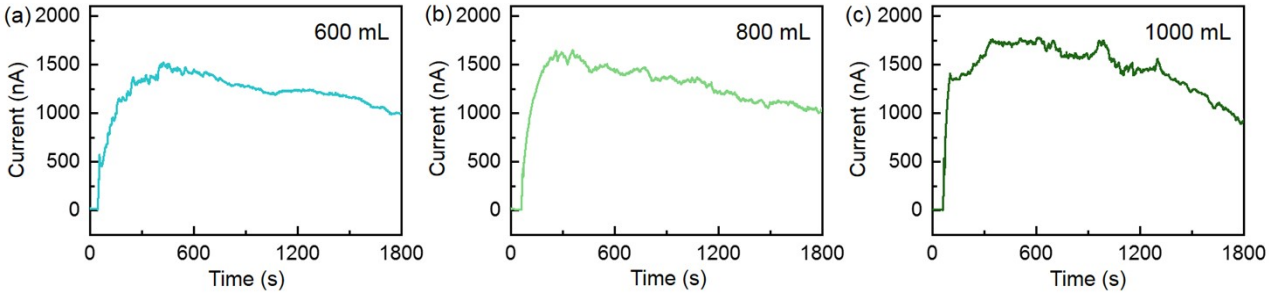

Fig. S17 Real-time current curve of the humidity sensor attached to diaper soaked with 600, 800 and 1000 mL.

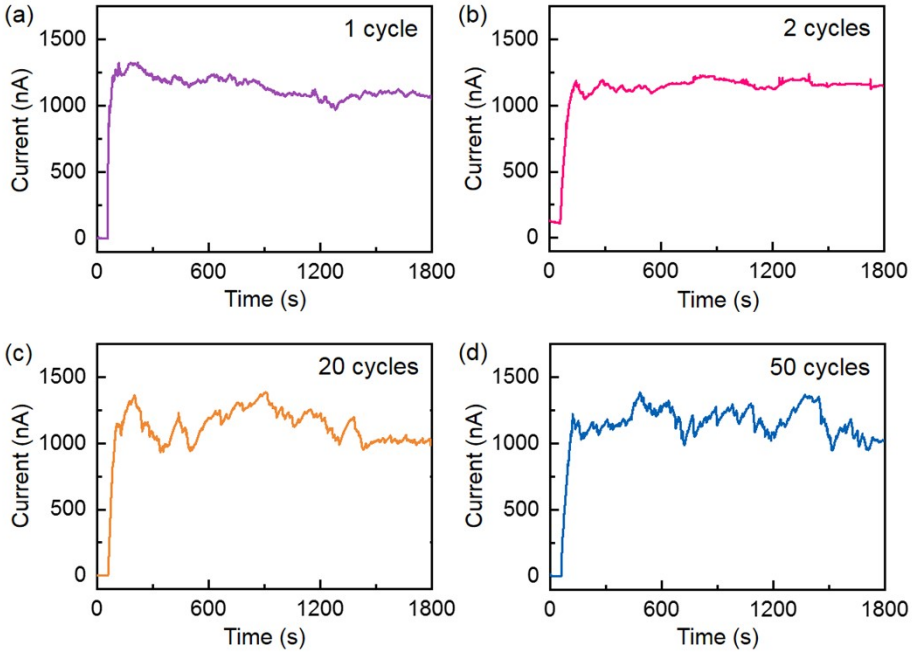

Fig. S18 Real-time current curve of the humidity sensor attached to diaper soaked with 500 mL of water at different cycles.

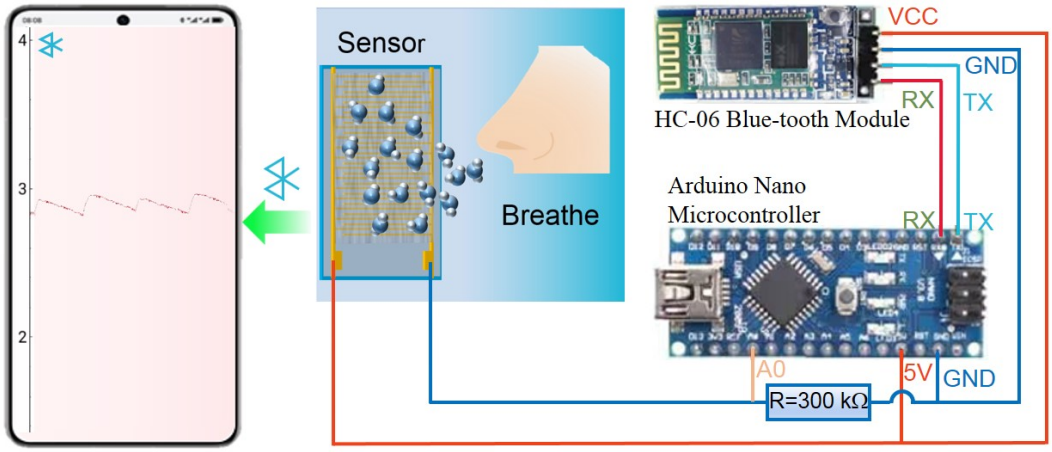

Fig. S19 Schematic illustration of wireless monitoring system of respiratory behavior.

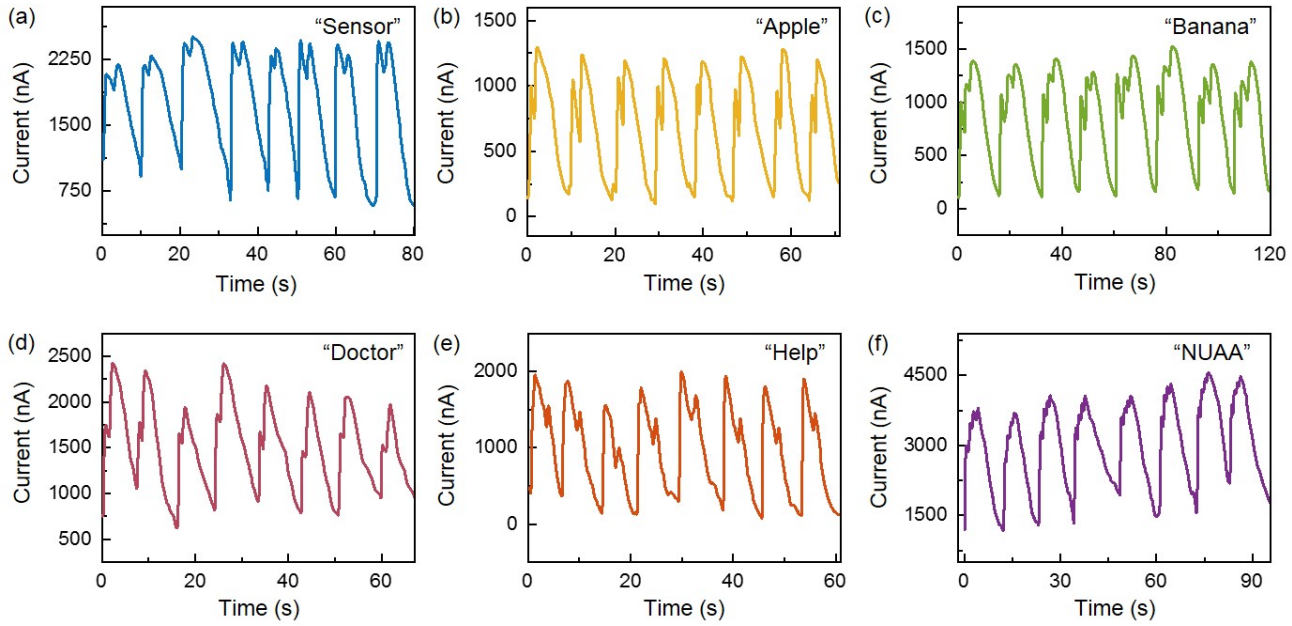

Fig. S20 Repeated responses of the humidity sensor to words: (a) ‘‘Sensor’’, (b) ‘‘Apple’’, (c) ‘‘Banana’’, (d) ‘‘Doctor’’, (e) ‘‘Help’’ and (g) ‘‘NUAA’’.

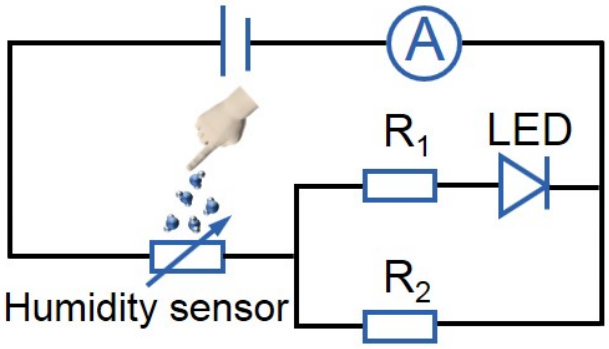

Fig. S21 Circuit diagram of the non-contact switch sensing system.

Tab. S1 The conductivity of the borophene-BC_2N heterostructures.

	Test 1	Test 2	Test 3	Test 4	Test 5	Test 6	Test 7	Test 8	Test 9	Test 10	Average	
Sample 1	329	381	361	378	368	394	396	394	382	390	377.3	
Sample 2	411	397	375	386	402	366	387	368	425	399	391.6	375.4
Sample 3	319	350	381	326	336	334	395	384	361	388	357.4	

Notes: the unit of conductivity is μs/cm

Tab. S2 Comparison of reported resistive humidity sensors.

Material	Measured RH Value	Sensitivity (%)	Response (s) / Recovery (s)	RH range (%)	Reference
Graphene	96	0.3	0.6/0.4	1-96	1
rGO	100	20.4	180-300/ Irreversible	10-100	2
MoS_2	89.5	2327	140/80	17.2-89.5	3
α′-4H-Borophene	85	150	2.3/0.7	67–85	4
Black phosphorus (BP)	97	521	101/26	11-97	5
rGO-PVP	90	52	10/20	20-90	6
rGO-MoS_2	50	23.9	30/253	10-90	7
rGO-SnO_2	95	4600	10/60	11-95	8
Borophene-graphene	85	4200	10.5/8.3	0-85	4
GO-C_{60}	97.3	1060	8/7	11.3-97.3	9
Borophene-BC_2N	**97**	**22001**	**11.82/1.41**	**11-97**	**This work**

References

1 A. D. Smith, K. Elgammal, F. Niklaus, A. Delin, A. C. Fischer, S. Vaziri, F. Forsberg, M. Rasander, H. Hugosson, L. Bergqvist, S. Schroder, S. Kataria, M. Ostling and M. C. Lemme, *Nanoscale,* 2015, **7**, 19099-19109.

2 D. Zhang, J. Tong and B. Xia, *Sensors and Actuators B: Chemical*, 2014, **197**, 66-72.

3 Y. Tan, K. Yu, T. Yang, Q. Zhang, W. Cong, H. Yin, Z. Zhang, Y. Chen and Z. Zhu, *J. Mater. Chem. C*, 2014, **2**, 5422.

4 C. Hou, G. A. Tai, B. Liu, Z. Wu and Y. Yin, *Nano Res.*, 2021, **14**, 2337-2344.

5 B. Li, Q. Tian, H. Su, X. Wang, T. Wang and D. Zhang, *Sensors and Actuators B: Chemical*, 2019, **299**, 126973.

6 B. Bhangare, S. Jagtap, N. Ramgir, R. Waichal, K. P. Muthe, S. K. Gupta, S. C. Gadkari, D. K. Aswal and S. Gosavi, *IEEE Sens. J.*, 2018, **18**, 9097-9104.

7 S. Y. Park, J. E. Lee, Y. H. Kim, J. J. Kim, Y. Shim, S. Y. Kim, M. H. Lee and H. W. Jang, *Sensors and Actuators B: Chemical*, 2018, **258**, 775-782.

8 M. B. Erande, M. S. Pawar and D. J. Late, *ACS Appl. Mater. Interfaces*, 2016, **8**, 11548-11556.

9 V. Shukla, J. Wärnå, N. K. Jena, A. Grigoriev and R. Ahuja, *J. Phys. Chem. C*, 2017, **121**, 26869-26876.